

Neutron Reflectometry of Quaternary Gemini Surfactants as a Function of Alkyl Chain Length: Anomalies Arising from Ion Association and Premicellar Aggregation

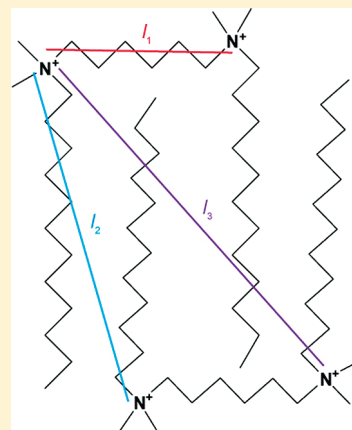
Pei Xun Li,^{*,†} Chu Chuan Dong,[†] Robert K. Thomas,[†] J. Penfold,[†] and Yilin Wang[§]

[†]Physical and Theoretical Chemistry Laboratory, South Parks Road, Oxford OX1 3QZ, United Kingdom

[‡]STFC, Rutherford-Appleton Laboratory, Chilton, Didcot, Oxfordshire OX11 0RA, United Kingdom

[§]Key Laboratory of Colloid and Interface Science, Institute of Chemistry, Chinese Academy of Sciences, Beijing 100090, China

ABSTRACT: We have measured the structure and properties of a series of dicationic quaternary ammonium compounds α,ω -bis(*N*-alkyl dimethyl ammonium)hexane halides ($C_n-C_6-C_n$) for values of the alkyl chain length n of 8, 9, 10, 11, 12, and 16, and a series of α,ω -bis(*N*-alkyl dimethyl ammonium)diethylether halides ($C_n-C_2OC_2-C_n$) for values of n of 8, 12, and 16, as well as $C_8-C_{12}-C_8$ and $C_{12}-C_{10}-C_{12}$ at the air/water interface. Although the critical micelle concentration (CMC) in the two series decreases in the normal way, that is, logarithmically, with increasing chain length, the limiting surface tension at the CMC and the limiting area per molecule both increase with chain length, in the opposite direction from comparable single chain surfactants. The structures of the surface layers, which were determined by neutron reflectometry, indicate that the anomalous behavior of the surface tension and area are probably caused by poor packing of the gemini side chains between adjacent molecules. Comparison of the directly determined surface coverage using neutron reflectometry and the apparent coverage determined by application of the Gibbs equation to surface tension data gives an experimental measurement of the prefactor in the Gibbs equation, which should be 3 for these geminis. It was found to vary from about 3 for the two C_{16} geminis down to about 1.5 for the two C_8 geminis. We have devised a simple quantitative model that explains this variation and earlier observations that the Gibbs prefactor for $C_{12}-C_n-C_{12}$ (n varying from 3 to 12) is around 2. The model is consistent with the conductivity, NMR, and fluorescence measurements of other authors. This model shows that both dimerization and ion association are required to explain the surface tension behavior of cationic gemini bromide surfactants and that, in many cases, the prefactor itself varies with concentration.



INTRODUCTION

The most widely studied series of gemini surfactants is the set of dicationic quaternary ammonium compounds α,ω -bis(*N*-alkyl dimethyl ammonium)alkane halides, $C_n-C_m-C_m$, where n and m , respectively, denote the number of carbon atoms in the chains of the free alkyl chain and the spacer. At the air–water interface, the adsorption behavior is mainly determined by the strong hydrophobicity of the two alkyl chains, but as the hydrophobic spacer length increases, it also starts to influence the adsorption. Surface tension measurements indicate that the area per molecule for $n = 12$ passes through a maximum at $m = 10–12$.¹ However, results from neutron reflectometry disagree with the surface tension results,² and this casts doubt on the use of surface tension data for the determination of the adsorption isotherm for this type of molecule. The problem is that the use of the Gibbs equation to obtain the surface excess requires assumptions about the state of association of the gemini and its counterions in the bulk solution. For full ionic dissociation and no premicellization, the prefactor in the Gibbs equation should be 3. However, use of the factor 3 leads to areas per molecule that

are unrealistically large relative to the molecular size and high surface activity of the geminis. Neutron reflectometry (NR) measures the surface excess directly with no assumptions, and measurements for the series $C_{12}-C_m-C_{12}$ do indeed give smaller, more plausible limiting areas than those obtained from the application of the prefactor 3 to the surface tension data. The correctness of the NR result for the air–water interface is reinforced by the values obtained by NR for the adsorption of these geminis at the silica–aqueous and hydrophobic–aqueous interfaces.³ The surface tension method with a prefactor of 3 gives values of 98 (105), 143 (143), and 224 (226) Å² for the $C_{12}C_mC_{12}$ dimethylammonium bromide geminis with spacers C_3 , C_6 , and C_{12} , respectively, where the values are from Li et al.² and Alami et al.¹ (values in brackets), whereas the neutron values are 78, 104, and $139 \pm 5\%$ Å², respectively. The corresponding values for the same geminis at the hydrophobic octadecyltrichlorosilane

Received: November 19, 2010

Revised: January 1, 2011

Published: February 01, 2011

(OTS) coated surface and the hydrophilic silica surface are 70, 85, and 98 Å² for OTS and 66, 84, and 110 Å² for the hydrophilic surface.³ The values at these two interfaces are smaller than those at the air–water interface, probably because both of these surfaces essentially create more hydrophobic environments, though in different ways from each other. The sources of experimental error and the few assumptions that need to be made in the interpretation of the NR data at the three interfaces are completely different, and the agreement between them therefore reinforces the reliability of the original NR result.

Comparison of the values of the coverages obtained from neutron reflection with those from surface tension on its own indicates that the Gibbs prefactor is usually significantly less than 3, which means that the geminis must either form premicellar aggregates and/or associate with their counterions. Zana⁴ has used electrical conductivity measurements to assess the state of ionization or premicellar aggregation in several gemini systems and has concluded that the former is dominant for small geminis, for example, C₈–C₆–C₈ and that the latter is dominant for large geminis, for example, C₁₆–C₆–C₁₆. This would be consistent with short or long geminis having Gibbs prefactors less than the theoretical value of 3, as suggested by the conflict between neutron and surface tension results. However, Zana concluded that neither preassociation nor premicellar aggregation occurs in the intermediate range, for example, C₁₂–C₆–C₁₂, and therefore the large discrepancy between the two types of measurement apparently remains unexplained. Zana has suggested that the disagreement could be accounted for by discrepancies associated with ionic impurity, but without giving any explanation. At present, there is only one system, C₁₂–xylyl–C₁₂, where electrical conductivity, surface tension, and neutron reflectometry agree that there is no association of any kind. For this system, neutron reflectometry and surface tension give identical coverages if the Gibbs prefactor is taken to be 3.

We now extend our characterization of the surface properties of cationic geminis to C_n–C₆–C_n and C_n–C₂–O–C₂–C_n (C_n–E–C_n), with *n* varying from 8 to 16, using surface tension and neutron reflectometry. The critical micelle concentrations (CMCs) in this series decrease rapidly with increasing chain length, and, as pointed out by Zana, both incomplete dissociation into ions and premicellar association are very sensitive to concentration and therefore the Gibbs prefactor at the CMC for this series should also be very sensitive to the value of the CMC. A no less interesting question is how gemini surfactants arrange themselves at surfaces, particularly with regard to the location of the spacer at the interface. A previous paper examined the effect of spacer length on this structure,⁵ and here we extend the work to varying alkyl chain lengths.

EXPERIMENTAL METHODS

The deuterated gemini surfactants were prepared using the method of Menger and Littau.⁶ In this method, the temperature is kept below about 40 °C. A large excess of alkyldimethylamine was reacted with dibromoalkane (or dibromodiethylether) in warm acetone until precipitation of the α,ω-bis(*N*-alkyl dimethyl ammonium)alkane dibromide was complete. Chain-deuterated alkyldimethylamines were prepared by direct reaction of deuterated bromoalkane with dimethylamine in methanol. Bromoalkanes were prepared by reduction of alkanic acids with LiAlD₄ to give alkanol followed by bromination of the alkanol.⁷ Fully deuterated dibromoalkanes were prepared in the same way as the bromoalkanes but starting with the appropriate diacid. All compounds were purified by recrystallization from a mixture of ethanol and ethyl

acetate, with the ratio of the two varying according to the compound. The fully protonated surfactants were prepared in exactly the same way. The purity of the compounds was assessed from surface tension measurements and comparison with known values of the critical micelle concentrations. The results are in good agreement with measurements by others.^{1,8–11} No minima were observed in the surface tension versus $\ln c$ plots.

All the glassware and PTFE troughs were cleaned by soaking them in alkaline detergent overnight and then rinsing several times with ultra-pure water (Elgastat UHQ, Elga, U.K.). Surface tension measurements were made on a Krüss K10T digital tensiometer using the du Noüy ring method with a Pt/Ir ring. Before each measurement, the ring was rinsed with pure water and flamed to remove contaminants. The temperature was maintained to within 0.2 K. The neutron reflection measurements were carried out on the reflectometers CRISP and SURF at Rutherford Appleton Laboratory (Didcot, U.K.). The instruments and the procedure for making the measurements have been fully described elsewhere.¹²

RESULTS

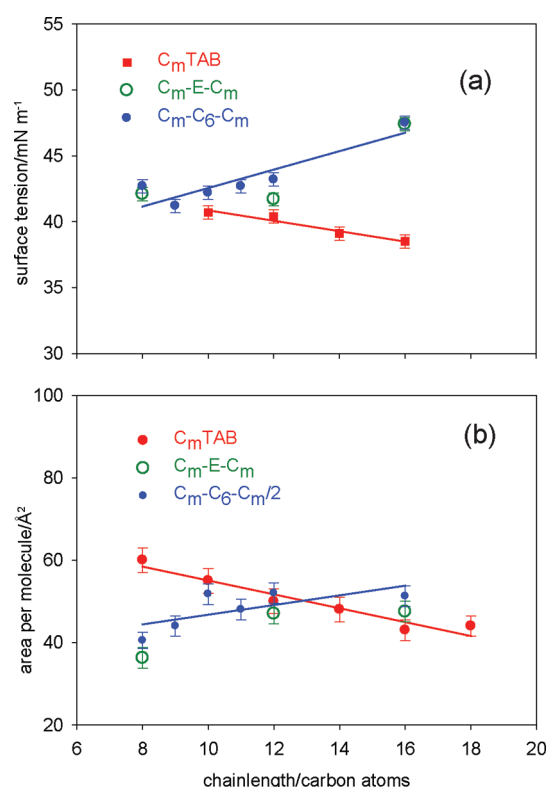
Surface Tension. Surface tension data were used to determine the CMCs and the limiting area per molecule at the CMC, assuming the Gibbs prefactor for complete dissociation, that is, 3 in the absence of NaBr and 1 at constant NaBr concentration. The values of these and the limiting surface tension are summarized in Table 1. The CMCs are in line with expectations for the increase in hydrophobicity with chain length, except for the C₈–C₆–C₈ compound; that is, $\log(\text{CMC})$ varies linearly with chain length (the C₈–C₆–C₈ compound presents special problems which will be discussed below). However, the surface tension at the CMC unexpectedly decreases from 47.5 mN m^{−1} for C₁₆–C₆–C₁₆ to 41.5 mN m^{−1} for the C₈–C₆–C₈ compound. This pattern is the same for the three compounds with the ether spacer. To emphasize the strangeness of this result, we compare the limiting surface tension of this series of geminis with the limiting surface tension for the single chain TABs in Figure 1a. The limiting surface tensions for the latter decrease with increasing chain length (hydrophobicity) in accord with expectations that the surface tension is a measure of surface activity. The result for the geminis suggests that the shorter the chain length in this series of geminis, the more surface active the compound.

The results in the presence of electrolyte show the type of changes one would expect, that is, a large reduction in the CMC, a drop in the limiting surface tension, and a substantial decrease in the slope of the curve as the CMC is approached. We comment on the values of the limiting areas per molecule after consideration of the neutron results.

Neutron Reflection. We first focus on the simplest of the neutron experiments, those done on the deuterated or partially deuterated gemini in solution in null reflecting water (NRW). The reflected signal under these circumstances is directly related to the surface coverage of the surfactant ion without any assumptions about the state of ionization of the surfactant. The results are given in Table 1. For one of the compounds, C₁₂–C₆–C₁₂, the present value of 104 Å² is slightly larger than our previously published value.² This could arise from experimental error or because the experiments were done on different isotopic species, chain deuterated in the present experiments and fully deuterated in the previous ones. (It does appear more generally from the gemini results that perdeuterated hydrocarbon fragments are slightly more hydrophobic than their

Table 1. Adsorbed Areas per Molecule of Gemini Surfactants Determined from Neutron Reflectometry and Gibbs Prefactors Determined by Combining Reflectometry and Surface Tension

surfactant	$\gamma_{\text{lim}} \pm 0.5$ (mN m ⁻¹)	CMC $\pm 20\%$ (mM)	$A_s \pm 10\%$ (Å ²)	$A_{\text{NR}} \pm 5\%$ (Å ²)	prefactor ± 0.4
C ₈ -C ₆ -C ₈	42.7	20	183	81	1.7
C ₈ -E-C ₈	42.1	19	186	74	1.4
C ₉ -C ₆ -C ₉	4.2	21	93	88	2.4
C ₁₀ -C ₆ -C ₁₀	42.2	7.7	136	103	2.4
C ₁₀ -C ₆ -C ₁₀ (0.1 M NaBr)	37.8	0.7	89	99	1.1
C ₁₁ -C ₆ -C ₁₁	42.7	2.5	134	96	2.4
C ₁₁ -C ₆ -C ₁₁ (0.1 M NaBr)	36.4	0.16	150	102	0.7
C ₁₂ -C ₆ -C ₁₂	43.2	1.1	123	104	2.3
C ₁₂ -E-C ₁₂	41.7	1.3	138	94	2.4
C ₁₆ -C ₆ -C ₁₆	47.5	0.016	117	102	3.0
C ₁₆ -E-C ₁₆	47.4	0.079	99	95	3.2
C ₈ -C ₁₂ -C ₈	41.3	6.6	153	112	2.2
C ₁₂ -C ₃ -C ₁₂ ^a	36.8		98	66	2.0
C ₁₂ -C ₄ -C ₁₂ ^a	39.9	1.2	142	82	1.7
C ₁₂ -C ₄ -C ₁₂ (0.1 M NaBr) ^a	34.8	0.014	109	87	0.8
C ₁₂ -C ₁₀ -C ₁₂	43.0	0.32	220	112	1.5
C ₁₂ -C ₁₂ -C ₁₂ ^a	42.8	0.28	224	140	1.9

^a From Li et al.²**Figure 1.** (a) Values of the limiting surface tension for geminis C_m-C₆-C_m, with values of *m* from 6 to 16, and values for the single chain trimethyl ammonium bromides for chain lengths 10 to 16. (b) Values of the limiting areas per molecules at the CMC for the same surfactants as in (a) (half the limiting area for the geminis). In both cases, the lines are to guide the eye.

protonated counterparts.) However, if we adopt the average value of 100 Å², both are within the typical neutron reflectometry error of 5–7% and this is a much smaller difference than that

between the neutron reflectometry results and those from surface tension where $A_s = 143$ Å². The limiting areas per molecule, plotted in Figure 1b, change in parallel with the limiting surface tensions shown in Figure 1a; that is, the area per molecule decreases with chain length, and the geminis with the less hydrophobic chains appear to pack more closely at the surface. This trend is the same for the three geminis with the ether spacer and similar for measurements made at CMC/10 with a small upward shift of the minimum. For comparison, we also show the behavior of the limiting area per molecule for the single chain TAB surfactants. As for the limiting surface tension, the normal manifestation of higher surface activity, that the area per molecule decreases with increasing surface activity, seems to be contravened in this series of geminis.

We can use the neutron measurements of limiting surface coverage in combination with the limiting gradient of the $\gamma - \ln c$ plot to obtain experimental values of the prefactor in the Gibbs equation. These values are plotted in Figure 2a. Notwithstanding the large error in this determination (mainly due to errors in the measured slope of the surface tension curve), the values increase from below 1.5 at C₈-C₆-C₈ and C₈-E-C₈ to approximately 3 at C₁₆-C₆-C₁₆ and C₁₆-E-C₁₆. The values of the slope of the $\gamma - \ln c$ plot have been determined by taking the average of the values obtained by fitting a limiting straight line and by fitting a curve to the limiting region of the surface tension. The values given for compounds that are not part of the present series of measurements have been determined simply from linear fits. We have included one new neutron measurement in the series C₁₂-C_m-C₁₂ for the C₁₂-C₁₀-C₁₂ compound. The Gibbs prefactors for the C₁₂-C_m-C₁₂ series of geminis are plotted in Figure 2b, and these are all close to 2 within the experimental error but seem to show a slight decrease as the length of the spacer increases. Given that the Gibbs prefactor depends on the state of the molecule in the bulk solution, the results suggest that C₁₆-C₆-C₁₆ and related ether geminis are close to being fully dissociated in the bulk solution, whereas the short chain compounds are more highly associated. The state of association of the

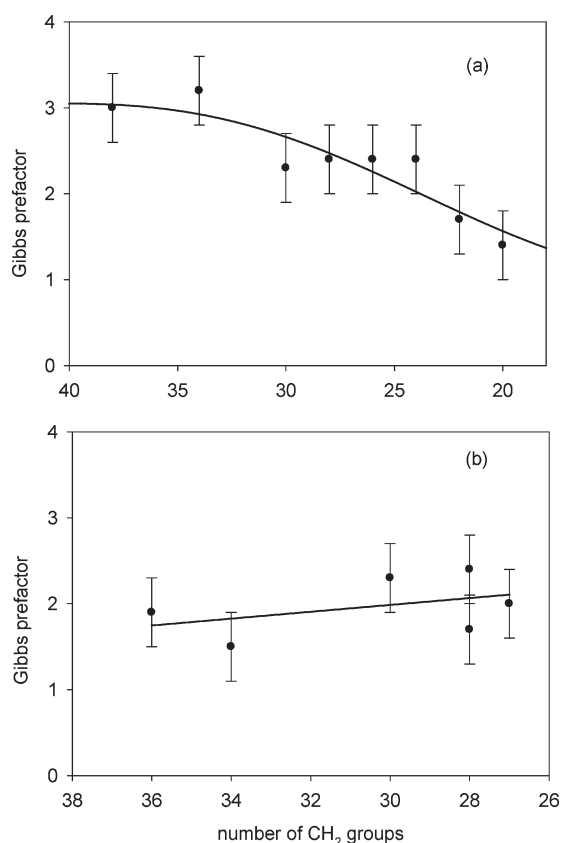


Figure 2. Experimentally determined Gibbs prefactors for (a) geminis with different length side chains and with C_6 or C_2OC_2 spacers and (b) geminis with different spacers (data mainly from Li et al.³). The line in (a) is the best fit of a polynomial with limits of 1 and 3 (the minimum and maximum values of the Gibbs prefactor corresponding to the maximum association from dimerization and ion association, most probable at high CMC, and complete dissociation, most probable at low CMC, respectively; see Table 3) and (b) is fitted with a simple straight line. However, both lines are just to guide the eye.

$C_{12}-C_m-C_{12}$ series seems to be relatively independent of spacer, but the previously observed value of about 2 for the prefactor for the $C_{12}-C_6-C_{12}$ compound now seems to be part of a consistent pattern.

The results on the surface coverage can be viewed in two ways. First, they show that determination of the surface excess from surface tension measurements is generally unlikely to give correct values and is often in error by up to 30%. Second, the comparison of neutron and surface tension results indicates that the origin of the error in the interpretation of the Gibbs equation lies in premicellar association, ion association, or both. If the interpretation of the origin of the error is correct, it is possible in principle to correct it if the state of submicellar aggregation of the gemini can be established quantitatively by independent means. Zana⁴ has shown that electrical conductivity measurements may elucidate the qualitative state of aggregation, and Warzyski et al.¹³ have suggested that ion electrode measurements might be more effective for quantitative measurement. However, quantitative interpretation from measurements of this type has not so far been possible, and the only correct values of the surface excess at present are then those determined by neutron reflectometry.

We also used isotopic substitution in conjunction with NR to determine the structure of the surfactant layers at the air–water

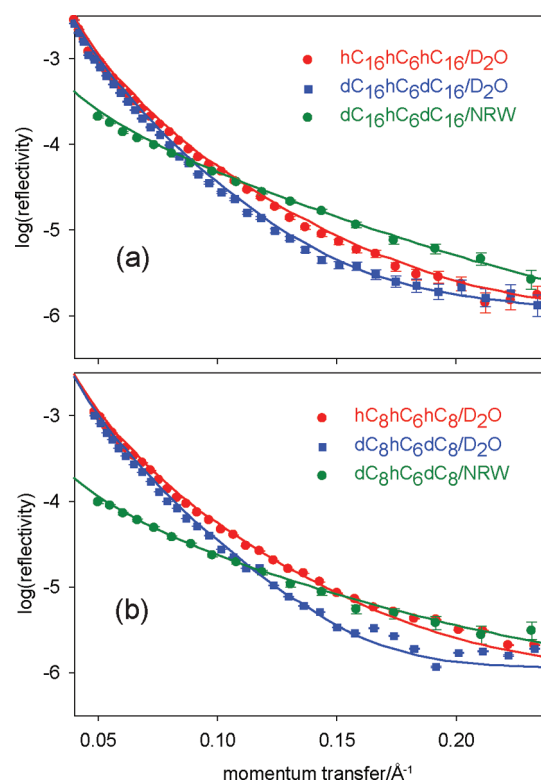


Figure 3. Neutron reflectivity profiles of three isotopic species of (a) $C_{16}-C_6-C_{16}$ and (b) $C_8-C_6-C_8$ with the best fits using the parameters in Table 2.

interface and in particular to identify the distributions along the surface normal of the components of the layer. We have done this for the series $C_n-C_6-C_n$ and C_n-E-C_n at the CMC and at CMC/10. These complement our earlier results on the $C_{12}-C_s-C_{12}$ series, but, in order to make a full comparison possible, we have reanalyzed the earlier data using the more refined fitting procedure developed for the present work. An adequate description of the structure is obtained from just three contrasts, $hC_n-hC_6-hC_n$ in D_2O and $dC_n-hC_6-dC_n$ in NRW and D_2O , rather than the five or six used in the earlier work. The fitted data for two geminis, $C_8-C_6-C_8$ and $C_{16}-C_6-C_{16}$, are shown in Figure 3, and the distributions for six selected gemini are shown in Figure 4. The data were fitted using the kinematic approximation and a division of the surface into the distributions of chains, heads, spacer, and water using methods described previously.¹⁴ The chains, heads, and spacers are described in terms of single Gaussian distributions defined by

$$f(z) = \left(\frac{2}{\sigma A \sqrt{\pi}} \right) \exp \left(-\frac{4z^2}{\sigma^2} \right)$$

where A is the area (\AA^2) per molecule and σ is the width of the distribution at $1/e$ of the maximum (taken to be the same for all three fragments). The water distribution is space-filling up to a certain cutoff and then decays as a half-Gaussian with the same width parameter as the other fragments.¹⁵ The Fourier transforms of these quantities are combined using the partial structure formalism to give the kinematic reflectivity,¹⁶ which is then corrected by the procedure devised by Crowley¹⁷ to give an accurate reflectivity profile for comparison with the data. As has been discussed previously, the results are most sensitive to the

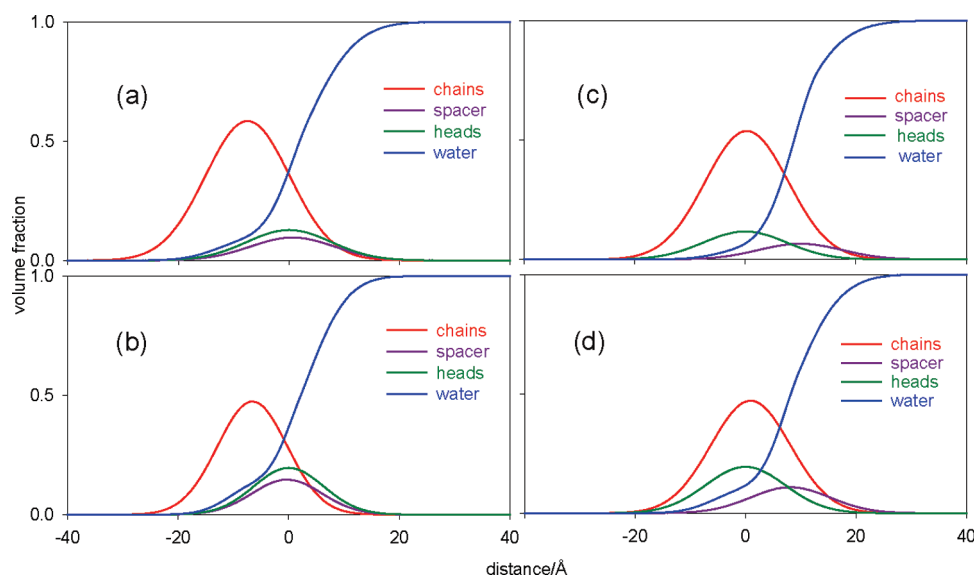


Figure 4. Distributions normal to the surface of water, chains, spacer, and head groups for geminis with C_6 and C_2OC_2 spacers: (a) $C_{16}C_6C_{16}$, (b) $C_8C_6C_8$, (c) $C_{16}EC_{16}$, and (d) C_8EC_8 .

Table 2. Characteristics of Adsorbed Layers of Gemini Surfactants at Their CMC at the Air–Water Interface^a

surfactant	$\sigma \pm 0.5$ (Å)	$\delta_{CW} \pm 0.5$ (Å)	$\delta_{SW} \pm 0.5$ (Å)	$\delta_{HW} \pm 0.5$ (Å)	$A \pm 3$ (Å)	$\tau \pm 1$ (Å)	$\Omega_{CW} \pm 0.03$	$\Omega_{SW} \pm 0.03$	$\Omega_{HW} \pm 0.03$
$C_{16}-C_6-C_{16}$	17	7.5	1.0	1.5	103		0.19	0.44	0.42
$C_{12}-C_6-C_{12}$	15	7.0	2.5	2.0	104	10.5	0.17	0.36	0.38
$C_{11}-C_6-C_{11}$	17	6.0	1.0	1.0	96		0.22	0.42	0.41
$C_{10}-C_6-C_{10}$	16	8.0	1.5	2.0	104		0.18	0.41	0.38
$C_9-C_6-C_9$	16	6.5	2.5	2.0	88		0.20	0.35	0.39
$C_8-C_6-C_8$	14	7.0	1.5	1.5	81		0.19	0.37	0.39
$C_8-C_{12}-C_8$	15	7.0	2.0	2.0	112		0.19	0.26	0.39
$C_{12}-C_3-C_{12}$	17.5	6.5	2.0	2.5	78	12.0	0.22	0.39	0.37
$C_{12}-C_4-C_{12}$	16.5	6.5	2.0	2.0	97		0.20	0.38	0.38
$C_{12}-C_{12}-C_{12}$	15	5.5	3.0	1.0	139	11.5	0.25	0.35	0.45
$C_{16}-E-C_{16}$	16	7.5	-3.5	2.0	95		0.15	0.68	0.42
$C_{12}-E-C_{12}$	15.5	7.0	-2.5	2.0	94		0.19	0.63	0.40
C_8-E-C_8	14	6.0	0.5	1.5	75		0.23	0.43	0.39

^a The errors quoted are relative ones; i.e., they only apply within the assumptions of the model.

area per molecule and the separations between the different fragment distributions. These are therefore the most accurately determined quantities. We have also calculated the overlap (Ω) between each of the three fragments and water by integrating over the product of the fragment and water distributions and then normalizing to the integrated fragment distribution.¹⁴ Because these depend primarily on the separations, they are also well determined in the experiment. The results for the measurements at the CMCs are given in Table 2 where the surfactants are grouped into the three basic series.

We first consider the results that are new to this paper, rather than the reanalyzed data. For each of the series $C_n-C_6-C_n$ and C_n-E-C_n , there is a small systematic decrease in σ with n . However, the effect is small in comparison with the change in the chain length. Exactly the same sort of change is shown by the single chain alkyl trimethylammonium bromides¹⁸ and is partly due to a large thermal roughness and partly due to a change in tilt angle with chain length. The large contribution of thermal roughness may be seen by comparing the values of σ with the

thickness of the layers at the hydrophobic solid/aqueous surface (τ) also included in Table 2 (note that σ and a uniform layer thickness are in theory not comparable but we have argued elsewhere that they are closer to a direct comparison than the width of the Gaussian at half-height¹⁹). A fully extended C_{16} chain is 21.7 Å long, whereas the C_8 chain is only 12.9 Å long. The thicknesses of the $C_{16}-X-C_{16}$ layers are substantially less than the fully extended chain length, indicating that the chains are strongly tilted away from the surface normal. On the other hand, there must be considerable roughness contributing to the thickness at least for the members of the two series with shorter chains because the layer is thicker than the fully extended chain length. An approximate estimate of the mean tilt angle can be obtained from $\theta = \cos^{-1}(2\delta_{CH}/l)$, where l is the fully extended length. This gives tilt angles centered on an average tilt angle relative to the horizontal of $33 \pm 5^\circ$ for $C_{16}-C_6-C_{16}$, $C_{16}-E-C_{16}$, $C_{12}-C_6-C_{12}$, and $C_{12}-E-C_{12}$, but this increases to an average of 48° for $C_8-C_6-C_8$, C_8-E-C_8 , and $C_8-C_{12}-C_8$. The chain/water overlap is not affected by these

differences in chain orientation and remains remarkably constant at about 0.2.

The spacer positions for the compounds with the E spacer are quite different from those with the C₆ spacers. The spacer is now somewhat hydrophilic and, as expected is more embedded in the water. This can be seen from the distribution of C₁₆–E–C₁₆ in Figure 4. It is also clearly seen from either the values of δ_{SW} or the relative values of Ω_{SW} to Ω_{HW} in Table 2. The effect is reduced at C₈–E–C₈. Part of the driving force for immersing the E spacer more fully in the water must be its greater hydrophilicity. However, the reduced effect for C₈–E–C₈ indicates that the E spacer is more squeezed out of the layer with the longer side chains. This idea is supported by the fact that the E spacer is no longer displaced in the direction of water at CMC/10 for any of the three compounds studied. There has been much discussion over the role of the spacer in determining the packing at the surface and whether or not it generates a maximum in the area per molecule. Diamant and Andelman modeled the C₁₂–C_m–C₁₂ series and showed that the presence of such a maximum depends on how the energy of the spacer is affected by its interactions with water.²⁰ This effect can be seen by comparing the overlaps Ω_{SW} and Ω_{HW} in Table 2. For all the C₆ and shorter spacers, Ω_{SW} and Ω_{HW} are identical within experimental error. However, for C₁₂–C₁₀–C₁₂, C₁₂–C₁₂–C₁₂, and C₈–C₁₂–C₈, Ω_{SW} decreases quite sharply relative to Ω_{HW} .

There is nothing immediately obvious in the variation of the structural data to explain why both the area per molecule and the limiting surface tension decrease with chain length in the series C_n–C₆–C_n. In single chain surfactants, the attractive interaction between longer hydrocarbon chains leads to a reduction of the limiting area per molecule with increasing chain length. Provided that the tilt of the chains does not change by too much and that the chains remain approximately aligned, this results in more effective screening of the water surface by a denser hydrocarbon layer and the limiting surface tension also decreases with increasing chain length. However, for the geminis, the decrease in area per molecule is up to about 20% over the range from C₁₆ to C₈ and the decrease in thickness is up to about 15%. Taking these maximum values gives a decrease of 38% in the volume occupied per surfactant to be compared with a decrease in the total volume of the surfactant (chains, spacer, and head group) of about 33%. On the face of it, these two values are within experimental error. However, as already mentioned, the thickness contains a large contribution from thermal roughness and this masks the true change in the intrinsic thickness. This means that the value of 38% will be a significant underestimate of the decrease in volume occupied per surfactant; that is, it can be concluded that the surfactant layer is significantly denser for the shorter chain length geminis. This is then the probable reason that the limiting surface tension is also lower for the shorter chain length geminis in this series. The reason for the denser packing may lie partly in the change in tilt angle of the chains. As shown above, the C₁₆ chains are on average tilted at $33 \pm 5^\circ$ to the horizontal, whereas the C₈ chains are at $48 \pm 5^\circ$. If, in addition, the chains are in a highly disordered orientational state, the molecules will increasingly push each other apart as the chain length increases. Thus, it seems that the spacer acts to prevent efficient packing of the chains at the surface, even when it is the more flexible spacer with a central oxygen atom. It is possible to argue that the effect may have an electrostatic origin. The CMC is much higher for the short chain geminis, and therefore, the electrostatic screening of the double charge at the surface should

be more effective and should reduce the lateral repulsion in the layer. However, this does not lead to comparable changes in the limiting area and surface tension of single chain surfactants, and the effect is experimentally negligible for three of the geminis in Table 1. It might also be plausible to argue that ion association, which is more prevalent in bulk solution for these geminis, could act to reduce the lateral repulsion and hence cause both limiting area and surface tension to decrease with chain length. However, ion association is a bulk effect, and it is difficult to see that the conditions at the surface will change very much with chain length.

For the structural parameters of the C₁₂–C_m–C₁₂ series, apart from the new results for C₁₂–C₁₀–C₁₂, we have reanalyzed the earlier data of Li et al. in a way that makes the neutron reflectometry results for all the geminis so far measured directly comparable. Li et al. found that there were weak features in the reflectivity profiles consistent with the presence of a small amount of an additional layer underneath the surface. Here we have used a lower resolution assessment of the data, and we did not find it necessary to include such a layer for the new data; we also found it possible to obtain adequate fits to the original data without such a layer. This leads to small differences in the overall thickness of the layer between the earlier results and those given in Table 2. It also leaves open the question of whether such a sublayer sometimes exists beneath the geminis at the air–water interface (see also the discussion in Khurana et al.²¹).

DISCUSSION

The results for the surface coverage of this series of geminis reinforce the correctness of the values of the limiting area per molecule obtained for the C₁₂C_mC₁₂ earlier obtained by Li et al. and indicate that the anomalous value of about 2 for the Gibbs prefactor in the same series is part of a systematic behavior associated with a combination of ion association and premicellization. We now examine that behavior in more detail.

Ion association and premicellization can be probed by electrical conductivity measurements. There are two main contributing factors. First, the conductivity will be reduced below its expected value if there is ion association because this reduces the current carriers in the solution. Plots of specific conductivity κ against concentration c or of equivalent conductivity Λ against $(c)^{1/2}$ will therefore deviate from their initial slopes toward lower gradients. Zana has observed this effect for cationic geminis with side chains lower than about 10 carbon atoms.⁴ The second factor of premicellar aggregation has a more complicated effect on the conductivity. Moilliet et al.²² argued that if a spherical ion of radius r forms an aggregate with m ions, its radius will increase to $rm^{1/3}$. From Stokes' law, the resistance to motion is proportional to the radius and hence drops from mr to $rm^{1/3}$ for the m separate ions, leading to an increase in the conductivity by a factor $m^{2/3}$. Thus, there should be a marked increase in the conductivity associated with premicellization. Secondary effects from ion interactions (Debye–Huckel, etc.) will come into play at either higher concentrations, that is, systems with higher CMCs, or when the aggregation number increases. For example, the pronounced drop in equivalent conductivity above the CMC is in the opposite direction and the break in slope is regularly used to determine both the CMC and the degree of ionization of the micelle. A maximum associated with premicellization was first observed by Moilliet et al.²² for methyl violet, but was more clearly established for the single chain surfactant octadecylpyridinium iodate and for the higher dialkyl dimethylammonium

bromides by Kraus et al.²³ Zana has also shown that such maxima also occur for the longer chain cationic geminis, that is, $C_{16}-C_8-C_{16}$.⁴ Thus, conductivity measurements can be used to infer the presence of premicellar aggregation. Since ion association occurs for the lower members of the symmetric cationic gemini series and premicellar aggregation occurs for the higher members, it is reasonable to suppose that both might occur for intermediate members of the series. The absence of observable effects of either in the conductivity may then indicate that neither occurs or that both occur and cancel each other. Zana has interpreted his results in terms of the former.

Earlier authors had postulated premicellar association on the basis of irregularities in the change of CMC with chain length or spacer.^{6,24} More recently, Jiang et al. have used NMR to show that in $C_{14}-C_s-C_{14}$ ($s \leq 4$) separate signals appear for monomer and preaggregate below the CMC, which is definitive evidence for premicellization.²⁵ For the $C_{12}-C_s-C_{12}$ ($s \leq 4$) series, an average signal shifting with concentration below the CMC is less direct but still strong evidence for premicellization in this series. The authors concluded that these compounds were forming premicellar aggregates at concentrations about half the CMC. You et al. have recently used fluorescence to examine the effects of NaBr on a series of geminis and have found evidence for premicellar association at higher electrolyte concentrations.²⁶ Mathias et al. have also used fluorescence to demonstrate premicellar association.¹⁰ Finally, Hattori et al.²⁷ have used neutron small angle scattering to show that the first change of slope in a C_8 chain gemini with an aromatic group spacer is associated with premicellization (this is related to the problem of correctly identifying the CMC for the $C_8-C_6-C_8$ compound mentioned above in that there are two break points in the surface tension curve, as found by Hattori et al.). This is interesting because most of the other examples focus on much longer chain geminis. As we will show below, although the tendency for short chain geminis to preaggregate is low, it can be strongly assisted by ion association, which becomes much more favorable at the higher CMC. However, none of the above studies seem to have included in their assessments any consideration of ion association, which is most clearly revealed in the conductivity measurements. The issue of the accuracy of conductivity experiments as a probe of these effects has been discussed by Warszynski et al. who have shown that measurement of the counterion concentration by an ion selective electrode should be more useful than a measurement of the conductivity.¹³ Warszynski et al. used a combination of a model isotherm and adjustable dissociation constants for ion association in the bulk solution to produce a self-consistent analysis of the surface tension data on a trivalent cationic gemini surfactant.¹³ Although not cast in terms of the Gibbs prefactor, such a calculation automatically includes a variation in this factor.

There is little discussion of how and why gemini surfactants might tend to associate with their counterions and to form premicellar aggregates, although the strong binding of counterions is an important feature of the isotherm devised by Warszynski et al. Given the shape of a gemini surfactant and given the need to minimize electrostatic repulsion, the most obvious simple structure is a dimer of the schematic form of Figure 5. This allows a reduction in the exposure of the hydrophobic groups to water, and the charge separation is a maximum. The electrostatic interaction in such a structure would be large. The crucial quantity is the ratio of the charge separation to the Bjerrum length (distance at which the electrostatic interaction

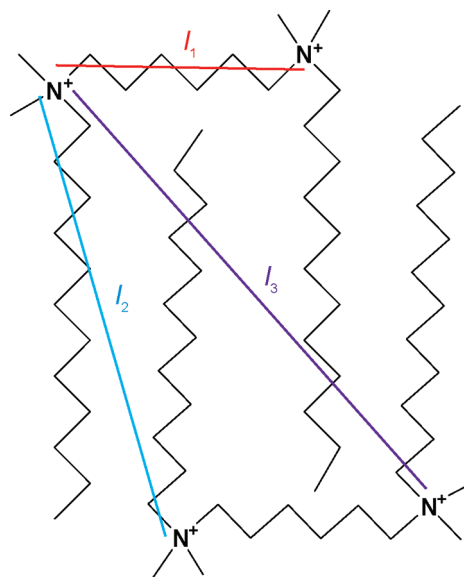


Figure 5. Schematic diagram of a gemini dimer.

energy is $k_B T$,²⁸ which is about 7 Å in water). If the gemini spacer is taken to be small enough that the charge at each end of the complex in Figure 5 is approximately 2^+ , the interaction between the doubly charged ends would have a Bjerrum length of 28 Å. This would make the electrostatic energy of the fully ionized dimer unreasonably high unless the dimer bound one counterion for chain lengths less about C_{20} , and two counterions for chain lengths less than about C_{10} . This suggests that dimerization and ion association must be coupled. As the spacer length increases, these conditions become less severe, but the presence of four charges is still associated with a large electrostatic energy. An additional possible factor is that the presence of so much low dielectric alkyl chain material may also change the effective dielectric constant from that of water. Two groups have considered the effect of the presence of low dielectric constant material in the vicinity of the charges in a system of two charged objects. Depending on how the alkyl chain material is distributed around the charges, the effective dielectric constant could vary from a value of 120, significantly above that of pure water, down to about 8.²⁹ The upper limit arises when the charges are opposite each other and lying on the outside of a sphere containing the low dielectric material, but this limit is unlikely to be achieved in the geminis because of the two methyl groups on each charged nitrogen. The lower limit applies when the charges are embedded toward the center of the sphere. Kornyshev et al.³⁰ have made a more refined calculation where the charges are embedded in an infinite cylinder of low dielectric with a variable diameter. Their results and the dimensions of the geminis suggest that the level of low dielectric material in a charged gemini dimer could enhance the tendency of the geminis to associate with one or more of their counterions by up to a factor of 15 relative to single charged species. Since ion association reduces the electrostatic repulsion in the dimer, it can be expected to assist dimer formation.

In Table 3, we tabulate limiting values for the prefactor in the Gibbs equation for the simple pattern of dimerization and ion association possible for the structure shown in Figure 5. Since association will change with concentration, the prefactor will vary across the surface tension curve, but the main emphasis of the

Table 3. Prefactors for Different Limiting States of Ionization and Association of Gemini Surfactants

ionization state	prefactor	prefactor in MX	$\lambda_{G_2^{4+}} = 2^{2/3}\lambda_{G^{2+}}$	$\lambda_{G_2^{4+}} = 2\lambda_{G^{2+}}$
$G^{2+} + 2X^-$	$g = 3$	$g = 1$	220	220
$GX^+ + X^-$	$g = 2$	$g = 1$	110	110
$G_2^{4+} + 4X^-$	$g = 5/2$	$g = 1/2$	260	280
$G_2X^{3+} + 3X^-$	$g = 2$	$g = 1/2$	190	240
$G_2X_2^{2+} + 2X^-$	$g = 3/2$	$g = 1/2$	130	140
$G_2X_3^+ + X^-$	$g = 1$	$g = 1/2$	65	70

neutron data is on the limiting coverage at the CMC and then it is appropriate to refer to a limiting value of the prefactor. We have included in Table 3 the values of the prefactor in excess electrolyte MX, where X is the gemini counterion, and values of the equivalent conductivity Λ for each state of ionization. The latter are estimated from the measurements by Zana⁴ as follows. The value of Λ for Br^- is known to be about 80 S cm²/mol, and hence, the value for a cationic gemini ion with a C₁₂ chain at infinite dilution can be estimated to be around 30 S cm²/mol from the overall value of about 220 S cm²/mol. According to the original argument of Moilliet et al., the conductivity of an associated gemini should be $3/2^{4/3}\lambda_{G^{2+}} + 3/2\lambda_{Br^-}$, which is about 190 S cm²/mol for a C₁₂ gemini. However, Zana's data for those geminis where the conductivity shows the strong increase characteristic of premicellization suggest that the increase of the conductivity of the gemini ion on dimerization may be higher than the $2^{2/3}$ factor proposed by Moilliet et al. Thus, the maxima in Λ reached by C₁₆–C₈–C₁₆ and C₁₈–C₈–C₁₈ are about 270 and 300 S cm²/mol, respectively, indicating that the increase might be better represented by a factor of 2. This would imply that the effective size of the gemini dimer with respect to diffusion is little different from the monomer. In this case, the value of Λ for the associated model of the fourth row of the table would be 240 S cm²/mol. The estimate for the ionization represented in row 4 of Table 3 therefore gives a range of possible values from 190 to 240 S cm²/mol, which straddles the value for complete dissociation. This suggests that the difference between the conductivity for a completely dissociated gemini and for one that forms a dimer associated with one counterion may be too small to be reliably distinguished in a conductivity measurement. Taken in conjunction with the fact that the surface tension and neutron measurements for C₁₂–C₆–C₁₂ can be made to agree if the Gibbs prefactor is close to 2, which is the prefactor appropriate for the ionization pattern in row 4 of Table 3, this strongly suggests that this gemini forms a dimer with one attached counterion in solution below the CMC. Further experimental evidence supporting this is that Pisarcik et al. obtained a value of the surface excess of 0.91×10^{-6} mol m⁻² in swamping electrolyte.³¹ This is almost exactly half the coverage obtained directly with neutrons, 1.75×10^{-6} mol m⁻². Although the neutron measurement for this particular compound was done in the absence of electrolyte, the effect of electrolyte on surface packing in three other related geminis is negligible at the CMC as shown in Table 1. Combination of this measurement with the neutron result therefore gives a prefactor of 1/2, which fits with the ionization scheme in row 4 but not that in row 1.

The conductivity measurements show unambiguously that ion association is present for the smaller geminis and premicellization is present for the larger geminis. Premicellization is driven by

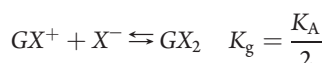
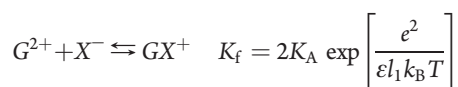
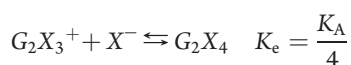
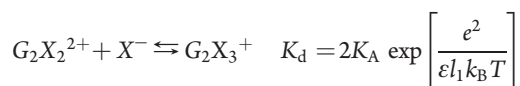
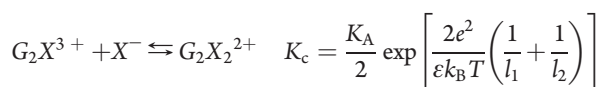
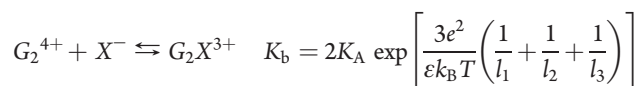
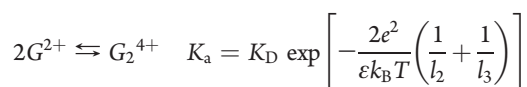
the hydrophobic effect and, for a given spacer length, should scale very approximately with the CMC. Close to the CMC, it should therefore be relatively independent of chain length; that is, it should be present at the CMC for most cationic geminis. In contrast, the equilibrium constant for ion association will intrinsically be independent of the gemini structure but ion association will increase with the CMC because of the higher ion concentration. In gemini dimers, ion association will also increase as the chain length decreases because the charge separation across the dimer decreases and it will show some dependence on the spacer. The conductivity measurements made by Zana can then be reinterpreted as follows. The data for a short chain gemini, C₈–C₆–C₈, was interpreted as ion association only. However, the values of the equivalent conductivity are too high to conform to the simplest ion association, row 2 of Table 1, being in the region of 150 S cm²/mol. They are more consistent with dimerization and association of two counterions to the dimer as would be expected from the arguments above. As the chain length increases and as the CMC drops, ion association will become weaker and, at the CMC of C₁₂–C₆–C₁₂, dimerization should still be significant but only one counterion needs to be attached to the dimer to reduce the electrostatic repulsion to a reasonable level. This gives a conductivity indistinguishable from the fully dissociated value but a Gibbs prefactor of 2 rather than 3, in agreement with the combination of neutron and surface tension measurements and with the NMR results of Jiang et al. At the longer chain lengths, dimerization remains strong but the tendency to associate a counterion disappears because of the low CMC and the greater charge separation. Dimerization is then dominant, leading to a sharp increase in the equivalent conductivity. This may be followed either by more extensive premicellization and/or ion association close to the CMC. One and/or the other of these must be responsible for the sharp downturn and the observed maximum. This was observed by Zana for C₁₆–C₈–C₁₆.

The results of Figure 2 and the values of the prefactor given in Table 3 show that the present series of surface tension and neutron reflectometry measurements on the C_m–C₆–C_m series of geminis are qualitatively consistent with these ideas. The effects of salt are less conclusive. Pisarcik et al. clearly found a value of 0.5 for the prefactor for C₁₂–C₆–C₁₂, which is exactly as expected for either dimerization or a combination of dimerization and ion association. However, our results for C₁₀–C₆–C₁₀, C₁₁–C₆–C₁₁, and C₁₂–C₄–C₁₂ give values of 1.1, 0.7, and 0.8, respectively. These are closer to 1.0 than to 0.5, although we again emphasize that the errors are quite large and particularly so as the gradient becomes flatter. The results of Li et al. on the C₁₂–xylyl–C₁₂ system then become the unusual ones.² This compound has a Gibbs prefactor of 3 showing that it is completely dissociated. There are three possible reasons for this exceptional behavior. First, the more rigid xylyl group may impose steric restrictions which make dimerization more difficult. Second, charge delocalization on to the xylyl group may weaken the electrostatic interaction with the counterions. Finally, the measurements on this compound were all performed at higher temperatures and this will reduce both types of association.

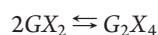
The problem with the interpretation of the surface tension data given above is that it only gives limiting values of the Gibbs prefactor, whereas in the real system the Gibbs prefactor will vary and will not necessarily reach any of the limits in Table 3 at the CMC. This has serious implications for the interpretation of the

slopes of γ - $\ln c$ plots. For example, the commonly observed situation that the coverage is more or less constant from say CMC/3 to the CMC will not give a straight line plot if the Gibbs prefactor is itself varying. Since the variation of surface tension when the Gibbs factor itself is varying also does not seem to have been considered previously, it is both instructive and important for the geminis to examine this quantitatively in terms of a simple model.

We assume the following set of equilibria, where G indicates a gemini, X a counterion and K_i the appropriate equilibrium constant.



where the K_a values are expressed in terms of a single ionassociation constant, K_A , and the dimerization constant of the uncharged gemini, K_D , which is the constant for



The inclusion of additional electrostatic contributions and statistical factors for the equilibria essentially follow the treatments of Bjerrum²⁸ and several other authors^{29,30,32–36} for the patterns of dissociation of dibasic organic acids and diamino bases. These are not strictly analogous because in those equilibria the charge disappears completely on association of the counterion, whereas it remains in the form of an ion pair here. We discuss this further below. There are also some other complications. The structure of Figure 5 would cause the equilibria above to split into several sub-branches, which would be difficult to handle without some simplification. To reduce this problem, the charges are therefore assumed to be on a rectangular framework of dimensions l_1 , l_2 , and diagonal l_3 . This reduces the number of branches in the equilibria to three, where the branching occurs at $G_2X_2^{2+}$. K_c and K_d are different for the three geometrically different species. The electrostatic terms are shown for one pair in the above reaction scheme and the others contain the analogous combinations of l_1 , l_2 and l_3 . Rather than treat the geometrically different $G_2X_2^{2+}$ as separate species, K_c and K_d are used as Boltzmann weighted averages. Following Ingold, the overall

surfactant concentration, c , is then given by

$$c = [G^{2+}] + [GX^+] + [GX_2] + 2[G_2^{4+}] + 2[G_2X_3^{3+}] + 2[G_2X_2^{2+}] + 2[G_2X_3^{3+}] + 2[G_2X_4]$$

and the electrical neutrality condition is

$$[X^-] = 2[G^{2+}] + [GX^+] + 4[G_2^{4+}] + 3[G_2X_3^{3+}] + 2[G_2X_2^{2+}] + [G_2X_3^{3+}] + [E]$$

where $[E]$ is the concentration of any added electrolyte and the difference between the three $G_2X_2^{2+}$ has been ignored. These equations can be solved numerically to give the concentrations of all the ions in the system and to give the change of each species with changes in the measured overall concentration of gemini, which are necessary for calculating the surface tension, for example,

$$\frac{d[G_2X_2^{2+}]}{dc}$$

The Gibbs equation can be written in terms of any set of independent components that make up the surface, for example, the doubly charged gemini ion and the counterion or the singly charged GX ion and the counterion.³⁷ Taking the former,

$$-d\gamma = RT\Gamma_{G^{2+}} \frac{d \ln[G^{2+}]}{d \ln c} d \ln c + RT\Gamma_{X^-} \frac{d \ln[X^-]}{d \ln c} d \ln c$$

where electrical neutrality requires that

$$2\Gamma_{G^{2+}} = \Gamma_{X^-}$$

Analytic forms of the Gibbs equation for the present set of equilibria could not be derived, although they can be for some simpler cases, for example, ion association only, dimerization only, or a restricted combination of the two. Here we use the neutron coverage data and numerical solution of the concentrations for trial values of K_A and K_D to predict the surface tension numerically. Where the neutron data cover the range of surface tension fitted, they were themselves fitted to a polynomial to obtain a finer grid for the calculation.

Premicellization has been a controversial issue in the literature, and there is little guidance for how K_D might vary between the geminis. We start with the simple assumption that K_a scales with the CMC. This has the effect that the extent of dimerization for all the geminis here is identical at their CMCs. There is some experimental information relating to K_A . Geng and Romsted³⁸ have measured the association constants for a short series of bolaform quaternary ammonium electrolytes, equivalent to the spacer part of the geminis. They obtained values of 16.7, 5.8, and 1.75 M⁻¹ for K_f (their K_1) for spacers of 2, 3, and 4 carbons, respectively. They also obtained a value of 0.83 M⁻¹ for the ionization of tetramethylammonium bromide (TMB⁺Br⁻), in line with other earlier measurements, and assumed that K_g (their K_2) has the same value of 0.83 M⁻¹. If the intrinsic association of the TMB⁺ ion pair is the same in the 1:1 as in the 2:1 electrolyte, then statistical factors would require K_g to be half that for the TM salt. This would give a value of only 0.4 M⁻¹. On the other hand, Geng and Romsted's result that K_g and the single ion dissociation are the same could also signify that the intrinsic binding in the bolaform is twice as strong as in the 1:1 electrolyte because of the statistical factor. To double K_g requires an additional attractive interaction equivalent to opposite charges at a distance of about

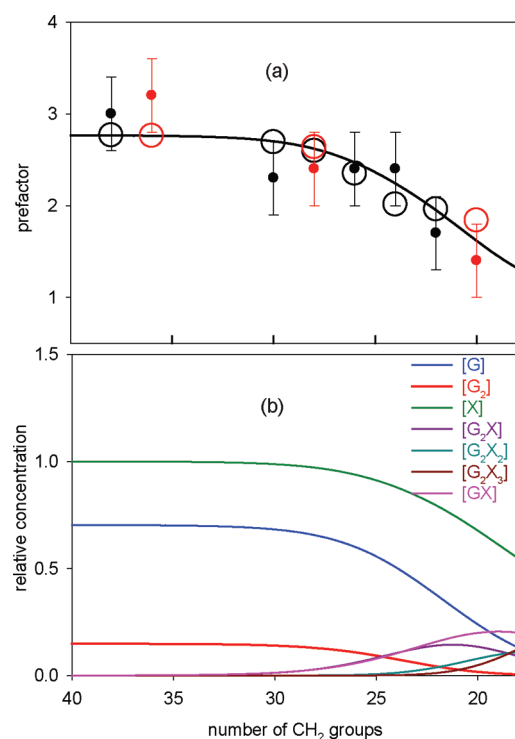


Figure 6. (a) Calculated (large circles and line) and observed (points) Gibbs prefactors at the CMCs for the series of C₆ and C₂OC₂ geminis for values of K_D and K_A of 0.3 and 0.8 M⁻¹. (b) The corresponding variation in the relative concentration of the different species in solution, also at the respective CMC. The limiting log CMC values are marked on the horizontal axis.

1 nm, which is plausible in these bolaforms because the bromide ion can interact specifically with one TM group on the bolaform while having an electrostatic attraction to the other at a larger distance. However, an additional interaction with the second charge would then cause K_g to vary with spacer length, which was not observed. This result implies that the electrostatic terms that we are using, based on complete neutralization, may be overestimates for the ion pairing system. In the end, the simplest strategy for fitting the data is to take the value of K_A to be as measured at 0.8 M⁻¹. The other important issue is the effective dielectric constant. Scharzenbach³⁶ has evaluated the effective dielectric constant acting between the charges in diaminoalkanes and shown that it varies smoothly from about 10 at a separation of 0.4 nm to 60 at 1 nm (compared with the standard bulk value for water of 78). For our geminis, the minimum distance corresponds to a value of about 40 and, since the variation between 40 and 70 was approximately linear in Schwarzenbach's data, we assume a similar linear relationship in our calculations. The theoretical work of Kornyshev et al. supports Schwarzenbach's conclusions, but it also shows that the matter is quite complex and the presence of the chains in the gemini could have a further effect on the effective ϵ . In addition, Blaak and Hansen³⁹ have shown that the effective dielectric constant may be different for interactions between like and unlike charges.

Figure 6 shows the numerical calculation (Newton–Raphson method for solution of the concentrations) of the Gibbs prefactor at the CMC for both series of geminis with C₆ and C₂OC₂ spacers. As in Figure 2a, the results are plotted against the total number of CH₂ and CH₃ fragments. The calculated values are

shown in two forms. The large circles are based on the measured CMC and the individual distances of each gemini (Figure 5). The line is approximate in that it assumes an empirical linear relation between side chain length and log CMC. Although this correlation is not perfect, the line fits the more accurately calculated points well when plotted against the total number of hydrophobic units. Reasonable fits to the whole set of nine geminis with just two parameters can be obtained with values of K_D and K_A of 0.3 and 0.8 M⁻¹ using the fully extended lengths of spacer and chain for l_1 and l_2 . The variation of the relative concentrations at the CMC (Figure 6b) show that only dimerization is significant for the longer chain compounds but at C₁₂ ion association creates significant amounts of G_2X^{3+} . This supports the suggestion above that the lack of any abnormalities in the conductivity of the C₁₂ series may result from a cancellation of the effects of dimer formation and ion association. At the lowest chain lengths, the gemini dimer is almost entirely in the form of G_2X^{3+} and $G_2X_2^{2+}$; that is, the relative reduction in conductivity is not due to association alone but to a complex mix of dimerization and dissociation. While the model gives a remarkably consistent explanation of the series of geminis with the fixed spacer, it does not explain the variation for varying spacer lengths in Figure 2b. All reasonable combinations of the parameters give a trend opposite to that observed. Note that for this series the effects are dominated by the value of the CMC. The only possible explanation is that dimerization or higher aggregation becomes relatively stronger as the spacer length increases. The configuration sketched in Figure 5 will become less favorable as the spacer length increases because it will increasingly allow the ingress of water. Either the geometry of the spacer will have to change or additional chains will have to be incorporated into the complex. Then either the stability of the dimer will change or higher aggregation will occur.

Figure 7 shows the calculation of the variation of the surface tension with $\ln c$ for C₁₁–C₆–C₁₁ (a) on its own and (b) with 0.1 M NaBr using the same pair of values of K_A and K_D as used for Figure 6. The fits of the experimental surface tension curves below the CMC and the concentrations of the important ions in the solution are shown. For completeness, the values of the surface tension above the CMC have been fitted independently by least-squares. The surface coverages in the absence of electrolyte were measured at four concentrations, from the CMC down to CMC/100, over which range the coverage exactly halved. The coverages were fitted to a quadratic in $\ln c$ for the calculation. The fits of the theoretical Gibbs prefactors of 3 and 1.0 (in red) are poor. However, the full calculation from the model gives good fits for both cases at the CMC for a single pair of values of K_A and K_D . In each case, the prefactor is varying significantly toward limiting values of 2 and 0.5, respectively, at the CMC. The model gives perfect agreement between the neutron and surface tension data in the absence of electrolyte, and it can be seen that the varying prefactor makes a significant contribution, generally tending to straighten out the curvature in the surface tension plot, which can be seen in the fixed prefactor calculation. The variation of the prefactor therefore partially cancels the effect of the changing coverage and extends the range over which a straight line can be fitted to the data. In these solutions, the dominant species are G^{2+} , G_2^{4+} and G_2X^{3+} ; that is, dimerization dominates but ion association of the dimer is significant. The presence of dimer will enhance the conductivity, but the formation of a significant level of G_2X^{3+} by ion association will offset this increase. We have not attempted to fit the

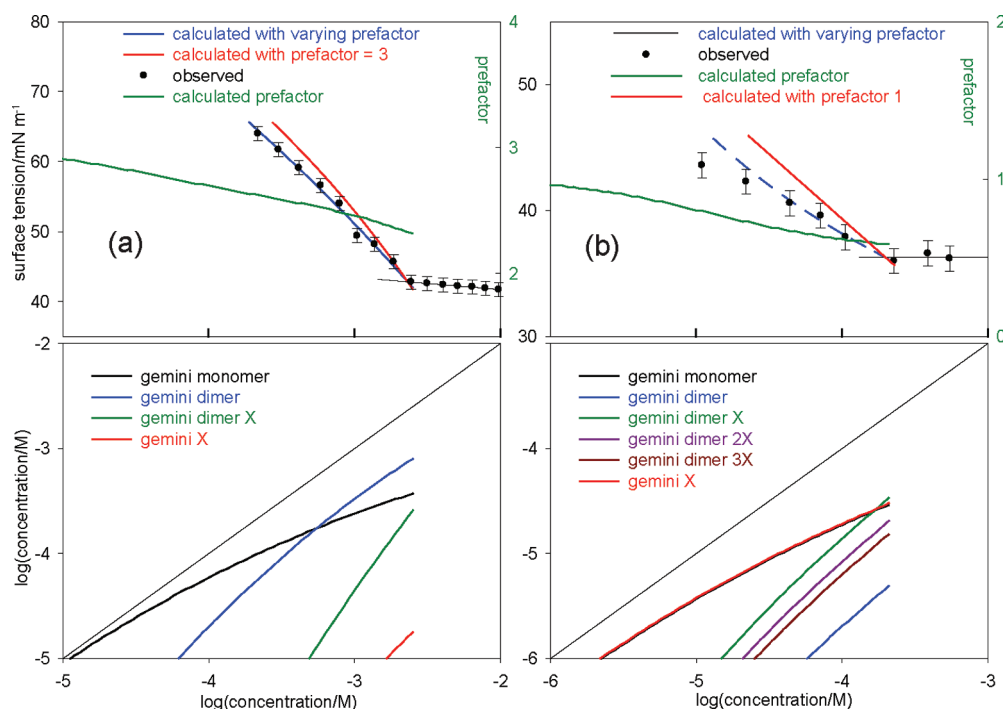


Figure 7. Calculated and observed surface tensions as a function of concentration for $C_{11}-C_6-C_{11}$ without (a) and with (b) added electrolyte (0.01 M) for values of K_D and K_A of 0.3 and 0.8 M^{-1} . The calculated surface tensions in (b) are based on a single measurement of the coverage at the CMC and so only extrapolate over a limited range toward lower concentrations. In (a), the coverage was measured at four concentrations and varied from 1.8 to $0.9 \times 10^{-6}\text{ mol m}^{-2}$ at the CMC and at CMC/100, respectively, and was fitted to the equation $\Gamma \times 10^6 = 6.07 + 107 + 1.03 \ln c + 0.05 \ln c^2$. In the lower parts of the graphs, the compositions of those species that occur at significant concentrations are also plotted. In (b), the coincidence of the concentrations of $[G]$ and $[GX]$ is itself a coincidence that only occurs at this concentration of electrolyte.

conductivity data partly because the calculation probably cannot be done accurately without use of the Debye–Hückel corrections and partly because the ion conductivities are difficult to estimate. For the electrolyte data, the coverage was only measured at the CMC; hence, only the higher concentration part of the curve can be fitted, but the correct gradient at the CMC is produced using the identical parameters as those used in the absence of electrolyte. This data (b) shows a quite different solution composition. The dominant ions are GX^+ and G_2X^{3+} , and the simple dimeric ion is insignificant. Thus, as anticipated in the discussion, dimerization is here assisted by ion association and this dominates the value of the prefactor, but there is some ion association to the single gemini ion.

CONCLUSIONS

We have shown that a model of combined dimerization and ion association can explain the differences in the surface coverages at the CMC measured by neutron reflectometry and by surface tension for cationic gemini surfactants. The model is consistent with a wide range of data and is also qualitatively consistent with conductivity, NMR, and fluorescence measurements. It also establishes that neutron reflectometry is the definitive method for measuring the coverage of geminis at the air–water interface and that, in situations where dimerization and/or association occur, the behavior of the surface tension with concentration may be more or less impossible to interpret quantitatively. The model was introduced to give some more solid support to qualitative arguments concerning the surface tension behavior. It seems to contain the minimum features to explain all the experimental observations.

We have shown two quantitative fits to the data: one to the whole series of experimentally derived prefactors in the Gibbs equation, and one to the surface tension data for $C_{11}C_6C_{11}$ with and without salt. Reasonable fits are also obtained for most of the other surfactants using values of K_D and K_A in the ranges 0.1 – 0.5 and 0.4 – 2.0 , respectively. However, for $C_{12}C_6C_{12}$, the calculated surface tension rises above the measured values at tensions above about 65 mN m^{-1} , and for the two C_{16} geminis the calculated surface tension falls below the observed values in the same high tension range. For the latter, the CMCs are very low and measurement of the surface tension becomes difficult at CMC/10 or lower. We have no certain explanation for the problem with $C_{12}C_6C_{12}$. It may be that the adsorbed layer breaks up into macroscopic islands at low coverages. This would cause the neutron measurement to overestimate the adsorbed amount, and since the adsorbed amount is used here to calculate the tension, the tension itself may then be overestimated. The range in the fitted values of K_D and K_A almost certainly results from too simple a model. The weaknesses of the model are (i) that dimerization varies in a less regular or different way from that assumed, (ii) the estimations of effective dielectric constant and its variation with distance, although based on an experimental study, are incorrect for the geminis, (iii) the dimerization structure may be different from Figure 5, and (iv) the electrostatic interaction may not be as strong for ion pairing as for complete association. None of these problems are easily solved.

The series of geminis $C_mC_6C_m$ and $C_mE_6C_m$ for values of m from 8 to 16 have the unusual properties that their limiting surface tension at the CMC and the limiting area per molecule both increase with chain length. This is attributed to the poor

packing of the gemini side chains at the surface. The longer the side chain, the more they interfere with each other and the less effective the screening of the high tension water surface.

AUTHOR INFORMATION

Corresponding Author

*E-mail: peixun.li@chem.ox.ac.uk.

ACKNOWLEDGMENT

P.X.L. thanks the Clarendon Fund of the University of Oxford for a scholarship. We thank Piotr Warszynski for a valuable conversation. We thank ISIS for the provision of neutron beam facilities. We thank the Royal Society, the Chinese Academy of Sciences, and the National Natural Science Foundation of China for support for collaboration between the Physical and Theoretical Chemistry Laboratory, University of Oxford and the Institute of Chemistry, Chinese Academy of Sciences, Beijing.

REFERENCES

- (1) Alami, E.; Beinert, G.; Marie, P.; Zana, R. *Langmuir* **1993**, *9*, 1465.
- (2) Li, Z. X.; Dong, C. C.; Thomas, R. K. *Langmuir* **1999**, *15*, 4392.
- (3) Li, P. X.; Dong, C. C.; Thomas, R. K. *Langmuir* **2010**, <http://dx.doi.org/10.1021/la104304y>.
- (4) Zana, R. *J. Colloid Interface Sci.* **2002**, *248*, 203.
- (5) Li, Z. X.; Dong, C. C.; Wang, J. B.; Thomas, R. K.; Penfold, J. *Langmuir* **2002**, *18*, 6614.
- (6) Menger, F. M.; Littau, C. A. *J. Am. Chem. Soc.* **1991**, *113*, 1451.
- (7) Furniss, B. S.; Hannford, A. J.; Smith, B. W. G.; Tatchell, A. R. *Vogel's Textbook of Practical Organic Chemistry*, 5th ed.; Longman: Essex, U.K., 1989.
- (8) Devinsky, F.; Lacko, I.; Mlynarcik, D.; Racansky, V.; Krasnec, L. *Tenside Deterg.* **1985**, *22*, 10.
- (9) Devinsky, F.; Lacko, I.; Bittererova, F.; Tomeckova, L. *J. Colloid Interface Sci.* **1986**, *114*, 314.
- (10) Rosen, M. J.; Mathias, J. H.; Davenport, L. *Langmuir* **1999**, *15*, 7340.
- (11) Zana, R.; Benraou, M.; Rueff, R. *Langmuir* **1991**, *7*, 1072.
- (12) Penfold, J.; Richardson, R. M.; Zarbakhsh, A.; Webster, J. R. P.; Bucknall, D. G.; Rennie, A. R.; Jones, R. A. L.; Cosgrove, T.; Thomas, R. K.; Higgins, J. S.; Fletcher, P. D. I.; Dickinson, E.; Roser, S. J.; McLure, I. A.; Hillman, A. R.; Richards, R. W.; Staples, E. J.; Burgess, A. N.; Simister, E. A.; White, J. W. *J. Chem. Soc., Faraday Trans.* **1997**, *93*, 3899.
- (13) Wegrzyska, J.; Para, G.; Chlebicki, J.; Warszynski, J.; Wilk, K. A. *Langmuir* **2008**, *24*, 3171.
- (14) Li, P. X.; Dong, C. C.; Thomas, R. K.; Wang, Y. L. *Langmuir* **2011**, *27*, 656.
- (15) Penfold, J.; Thomas, R. K. *Phys. Chem. Chem. Phys.* **2002**, *4*, 2648.
- (16) Lu, J. R.; Lee, E. M.; Thomas, R. K. *Acta Crystallogr., Sect. A* **1996**, *52*, 11.
- (17) Crowley, T. L. *Physica A* **1993**, *195*, 354.
- (18) Lu, J. R.; Thomas, R. K.; Penfold, J. *Adv. Colloid Interface Sci.* **2000**, *84*, 143.
- (19) Lu, J. R.; Simister, E. A.; Thomas, R. K.; Penfold, J. *J. Phys.: Condens. Matter* **1994**, *6*, A403–A408.
- (20) Diamant, H.; Andelman, D. *Langmuir* **1994**, *10*, 2910.
- (21) Khurana, E.; Nielsen, S. O.; Klein, M. L. *J. Phys. Chem. B* **2006**, *110*, 22136.
- (22) Moilliet, J. L.; Collie, B.; Robinson, C.; Hartley, G. S. *Trans. Faraday Soc.* **1935**, *31*, 120.
- (23) Evers, E. C.; Grieger, P. C.; Kraus, C. A. *J. Am. Chem. Soc.* **1946**, *68*, 1137.
- (24) Rosen, M. J.; Liu, L. T. *J. Am. Oil Chem. Soc.* **1996**, *73*, 885.
- (25) Jiang, Y.; Chen, H.; Cui, X. H.; Mao, S. Z.; Liu, M. L.; Luo, P. Y.; Du, Y. R. *Langmuir* **2008**, *24*, 3118.
- (26) You, Y.; Zhao, J. X.; Jiang, R.; Cao, J. J. *Colloid Polym. Sci.* **2009**, *287*, 839.
- (27) Hattori, N.; Hirata, H.; Okabayashi, H.; O'Connor, C. J. *Colloid Polym. Sci.* **1999**, *277*, 361.
- (28) Bjerrum, N. K. *Z. Phys. Chem.* **1923**, *106*, 219.
- (29) Kirkwood, J. G.; Westheimer, F. H. *J. Chem. Phys.* **1938**, *6*, 506.
- (30) Kornyshev, A. A.; Vorotyntsev, M. A.; Nielsen, H.; Ulstrup, J. *J. Chem. Soc., Faraday Trans.* **1982**, *78*, 217.
- (31) Pisarcik, M.; Rosen, M. J.; Polakovicova, M.; Devinsky, F.; Lacko, I. *J. Colloid Interface Sci.* **2005**, *289*, 560.
- (32) Gane, R.; Ingold, C. K. *J. Chem. Soc.* **1928**, 1594.
- (33) Gane, R.; Ingold, C. K. *J. Chem. Soc.* **1931**, 2153.
- (34) Ingold, C. K. *J. Chem. Soc.* **1931**, 2170.
- (35) Ingold, C. K. *J. Chem. Soc.* **1931**, 2179.
- (36) Schwarzenbach, G. *Pure Appl. Chem.* **1970**, *24*, 307.
- (37) Guggenheim, E. A. *Thermodynamics*, 5th ed.; North Holland Publishing Company: Amsterdam, 1967.
- (38) Geng, Y.; Romsted, L. S. *J. Phys. Chem. B* **2005**, *109*, 23629.
- (39) Blaak, R.; Hansen, J. P. *J. Chem. Phys.* **2006**, *124*, 144714.